Am J Physiol Gastrointest Liver Physiol 327: G140–G153, 2024.
First published May 23, 2024; doi:10.1152/ajpgi.00022.2024

american physiological society

AMERICAN JOURNAL OF PHYSIOLOGY
GASTROINTESTINAL AND LIVER PHYSIOLOGY

RESEARCH ARTICLE

Oral administration of CXCL12-expressing *Limosilactobacillus reuteri* improves colitis by local immunomodulatory actions in preclinical models

Emelie Öhnstedt,[1,2] Cristian Doñas,[1] Kristel Parv,[1] Yanhong Pang,[1] Hava Lofton Tomenius,[1,2] Macarena Carrasco López,[1] Venkata Ram Gannavarapu,[2] Jacueline Choi,[2] Maria Ovezik,[2] Peter Frank,[1] Margareth Jorvid,[1] Stefan Roos,[3] Evelina Vågesjö,[1,2] and Mia Phillipson[2,4]

[1]*Ilya Pharma AB, Uppsala, Sweden;* [2]*Division of Integrative Physiology, Department of Medical Cell Biology, Uppsala University, Uppsala, Sweden;* [3]*Department of Molecular Sciences, Swedish University of Agriculture, Uppsala, Sweden; and* [4]*The Science for Life Laboratory, Uppsala University, Uppsala, Sweden*

Abstract

Treatments of colitis, inflammation of the intestine, rely on induction of immune suppression associated with systemic adverse events, including recurrent infections. This treatment strategy is specifically problematic in the increasing population of patients with cancer with immune checkpoint inhibitor (ICI)-induced colitis, as immune suppression also interferes with the ICI-treatment response. Thus, there is a need for local-acting treatments that reduce inflammation and enhance intestinal healing. Here, we investigated the effect and safety of bacterial delivery of short-lived immunomodulating chemokines to the inflamed intestine in mice with colitis. Colitis was induced by dextran sulfate sodium (DSS) alone or in combination with ICI (anti-PD1 and anti-CTLA-4), and *Limosilactobacillus reuteri* R2LC (*L. reuteri* R2LC) genetically modified to express the chemokine CXCL12-1α (R2LC_CXCL12, emilimogene sigulactibac) was given perorally. In addition, the pharmacology and safety of the formulated drug candidate, ILP100-Oral, were evaluated in rabbits. Peroral CXCL12-producing *L. reuteri* R2LC significantly improved colitis symptoms already after 2 days in mice with overt DSS and ICI-induced colitis, which in benchmarking experiments was demonstrated to be superior to treatments with anti-TNF-α, anti-α4β7, and corticosteroids. The mechanism of action involved chemokine delivery to Peyer's patches (PPs), confirmed by local CXCR4 signaling, and increased numbers of colonic, regulatory immune cells expressing IL-10 and TGF-β1. No systemic exposure or engraftment could be detected in mice, and product feasibility, pharmacology, and safety were confirmed in rabbits. In conclusion, peroral CXCL12-producing *L. reuteri* R2LC efficiently ameliorates colitis, enhances mucosal healing, and has a favorable safety profile.

NEW & NOTEWORTHY Colitis symptoms are efficiently reduced by peroral administration of probiotic bacteria genetically modified to deliver CXCL12 locally to the inflamed intestine in several mouse models.

colitis; drug delivery; ILP100; immunotherapies; Limosilactobacillus reuteri

INTRODUCTION

The anatomy of the gastrointestinal (GI) tract allows for specific interactions between the intestinal microbiota and the numerous immune cells of the lamina propria. These bacterial-immune cell interactions are known to be important for host health, susceptibility to disease, and treatment response to immunotherapies (1–8). The Peyer's patches (PPs), lymphoid tissues in the distal small intestine, are in contrast to the rest of the GI tract covered by only a thin mucus layer, which allows for efficient sampling of the luminal content by subepithelial immune cells. As a consequence, luminal antigens activate B lymphocytes in the PPs, and the majority of the intestinal IgA important for shaping the intestinal microbiome is induced at this site (9). We have previously reported that peroral administration of *Limosilactobacillus reuteri* R2LC (*L.reuteri* R2LC), but not other *L. reuteri* strains, upregulates sphingosine-1-phosphate receptors (S1PRs) on subepithelial B lymphocytes in the PPs of mice, which results in strong IgA induction. Consequently, the population of IgA-producing B cells increases in the mucosa of both colon and ileum, resulting in more IgA released to the lumen, which shifts the gut microbiota of healthy and dextran sulfate sodium (DSS)-colitic mice into one associated with health when administered prophylactically (10–12).

Colitis encompasses several different forms with different etiologies and prevalences, including inflammatory bowel disease (IBD), as well as ischemic-, infectious-, and drug therapy-induced enteropathies. General treatment strategies rely on dampening immune cell activity or interfering with their trafficking to the intestine and include corticosteroids, which may be escalated to biologics such as anti-TNF and anti-α4β7 therapies (13–15). The biologics are administered intravenously and are associated with severe systemic side

Correspondence: M. Phillipson (mia.phillipson@mcb.uu.se).
Submitted 26 January 2024 / Revised 26 April 2024 / Accepted 2 May 2024

effects (16, 17). Despite gut-selective claims, the adverse event profile of even the most recent addition on the market mainly reports immune-related events in the lung as well as in additional organs outside of the GI tract (Vedolizumab, an anti-α4β7 therapy, 18). Recently, an S1P modulator (Ozanimod) was repurposed from the original indication for multiple sclerosis and approved for ulcerative colitis (UC) treatment, where inflammation is reduced by retaining immune cells in the lymphoid tissues. However, this treatment is associated with adverse events, of which those reported as common (1/100–1/10) include lymphopenia, bradyarrhythmia, and elevated liver enzymes (19–21). In addition, all systemic immunosuppressive therapies are associated with systemic side effects, including infections, and approaches to acquire only local effects as well as to promote mucosal healing without suppressing the immune system would be a very attractive choice to patients (13, 16, 17, 22). Peroral administration of probiotics to patients with colitis has shown mixed outcomes, where some evidence indicates reduced disease activity but not remission in UC (23) even though the underlying mechanism remains elusive. Of interest, we recently found that peroral pretreatment with specifically *L. reuteri* R2LC reduced disease activity in an S1P- and IgA-dependent manner in mice with DSS-induced colitis (10).

Immune checkpoint inhibitors (ICIs) have transformed treatment options for patients with cancer and produce robust and durable remissions in a variety of malignancies, such as skin, breast, bladder, and colon cancers (24). As ICI therapy acts by blocking the inherent regulation of the immune system, immune-related adverse events are common and force up to 25% of patients to discontinue treatment (25). The most common immune-related adverse event is colitis (referred to as ICI-induced colitis), which occurs in up to 57% of all patients where 10% develop severe colitis necessitating interruption of ICI treatment (26, 27). For these individuals, local-acting therapies to ameliorate inflammation and increase mucosal healing without impairing the therapeutic effect of tumor-targeting immunotherapy would widen the therapeutic window and allow continued anticancer treatment.

The aim of the current study was to test if we could develop a local-acting immunotherapy that ameliorates colitis by enhancing mucosal healing without interfering with the systemic immune responses for the most relevant target population. Thus, the therapeutic potential of *L. reuteri* R2LC genetically modified to express and locally deliver the chemokine CXCL12-1α (referred to herein as R2LC_CXCL12 and emilimogene sigulactibac) to ameliorate overt colitis was investigated in animal models of chemically induced (DSS) and immunologically induced colitis (using ICIs). We found that treatment with R2LC_CXCL12 in mice with colitis ameliorated the disease activity index (DAI) through local actions in the intestine, as no systemic effects or exposure of the bacteria or CXCL12 could be detected. Of importance, the effect size on DAI was demonstrated to be greater with R2LC_CXCL12 when compared with corticosteroids, anti-TNF, and anti-α4β7 therapies, and the onset of effect following the start of treatment was noted earlier. In addition, product feasibility and safety were further confirmed in rabbits using a formulated product with lyophilized R2LC_CXCL12 filled in capsules (ILP100-Oral).

MATERIALS AND METHODS

Study Design

The mice were divided into groups, where group of mice that presented the highest disparities in body weight at the beginning of the experiment was selected to be the healthy group receiving the vehicle only. Colitis was induced using 3% DSS (TdB laboratories)-water solution for 5 days (*day 1* to *day 6*), followed by normal tap water. The groups were evaluated based on DAI on *day 6* to ensure that the severity of colitis was similar between all groups exposed to 3% DSS solution when the different treatments started. The mice were then treated perorally with vehicle (freezing solution), WT_R2LC, R2LC_CXCL12, or prednisolone (PDS), or by intraperitoneal injections (anti-TNF-α or anti-α4β7) for 6 days (Figs. 1, *A* and *E*, and 2*A*).

In some experiments, DSS-treated mice were cotreated with ICI: anti-PD-1 (100 μg/mouse) (no. BE0146, BioXCell) and anti-CTLA-4 (100 μg/mouse, no. BE0164, BioXCell) or respective isotype controls IgG2a (no. BE0089, BioXCell) and IgG2b (no. BE0086, BioXCell) administered intraperitoneally every third day and started 3 days before DSS treatment (Fig. 3*A*). These mice were then treated perorally with vehicle, WT_R2LC, or R2LC_CXCL12 for 6 days.

To test the immediate effects of R2LC_CXCL12 on anti-PD1-induced colon ulcers, female BALB/c mice were inoculated with 4T1 cells in the mammary glands on *day 1* and thereafter treated with intraperitoneal injections of anti-PD1 or IgG2a isotype control on *days 8*, *15*, and *21*, followed by 7 days of a single-dose oral gavage with vehicle or R2LC_CXCL12. The 4T1 cells are highly metastasizing cancer cells known to have a weak response to anti-PD1 monotherapy.

To investigate the ability of R2LC_CXCL12 to induce IgA, healthy mice were treated with vehicle, WT_R2LC, or R2LC_CXCL12 once a day for 7 days.

Experimental Animals

Male C57Bl/6 mice (Taconic, Denmark or Charles River, Germany) and female BALB/c mice (Janvier Labs, France) were used at an age of 7–8 wk. All mouse experiments were approved by a Local Ethical Committee (no. C6/16, no. C03569/21, or no. M4392/2018 with amendment no. 5.8.18–17188/2018).

Male and female New Zealand white rabbits (Charles River) were used. Male rabbits were housed individually, and female rabbits were housed in socially compatible groups and only together with other animals belonging to the same treatment group. All rabbit experiments were approved by the Danish Veterinary and Food Administration (no. 2015-15-0201–00713).

Evaluation of Colitis

Disease progression was assessed using DAI, which is defined by loss of body weight, stool consistency, and blood in the stool or rectal bleeding following the criteria already established by Cooper et al., with some adjustments including a more extensive description of scores 2 and 4 for stool consistency and blood in feces (28). The percentage of body weight loss was defined by considering the weight on *day 1* as 100% of the body weight. Intestinal bleeding was evaluated by Hemoccult (positive signal: +) (TrioLab). Each mouse received a score corresponding to the average values of the three criteria as depicted in Table 1.

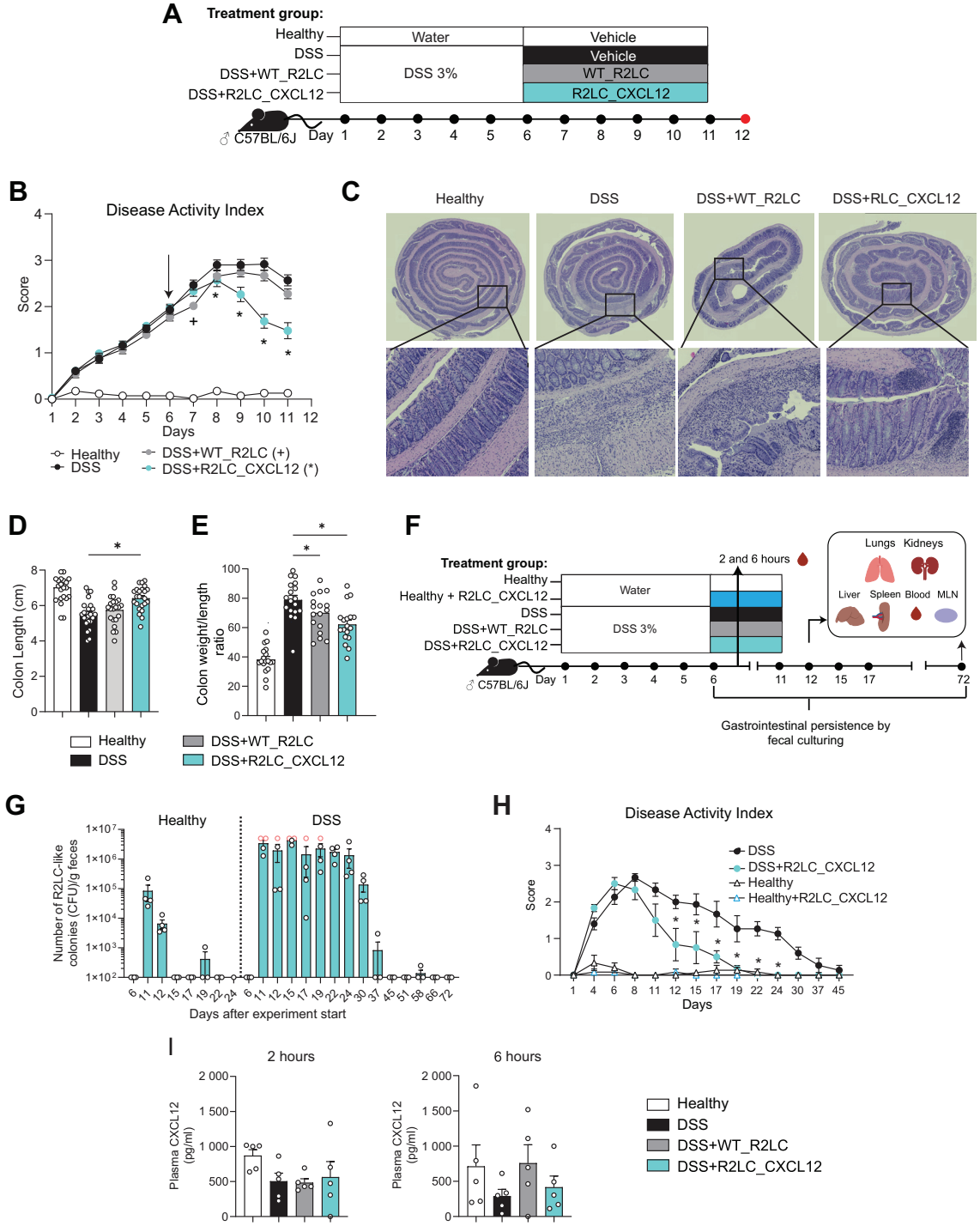

Figure 1. R2LC_CXCL12 ameliorates dextran sulfate sodium (DSS)-induced colitis. *A*: a schematic overview of the experimental design. Vehicle, WT_R2LC, and R2LC_CXCL12 were given by oral gavage (100 μL per dose; 2×10^9 CFU per dose; three times a day, and in four independent experiments). Arrow indicates start of treatment and red circle indicates the time point when mice were terminated. *B*: disease activity index (DAI) over time in all groups ($n = 23$ animals per group). *C*: representative images of hematoxylin and eosin-stained colonic tissue. *D*: colon length ($n = 22$ or 23 animals per group). *E*: weight-to-length ratio on *day 12* ($n = 17$ or 18 animals per group). *F*: schematic overview of the experiments designed to reveal exposure and gastrointestinal persistence of R2LC_CXCL12 in mice, as well as translocation to blood and inner organs [lungs, kidney, liver, spleen, and mesenteric lymph node (MLN)]. Vehicle, WT_R2LC, and R2LC_CXCL12 were given by oral gavage (100 μL per dose; 2×10^9 CFU per dose; three times a day in one independent experiment). *G*: persistence of R2LC_CXCL12 in feces of healthy and DSS-treated mice ($n = 5$ animals per group. Red outlined dots indicate samples where the plates had too many colonies to count, details in MATERIALS AND METHODS. *H*: long-term DAI follow up ($n = 5$ animals per group). *I*: plasma CXCL12 at 2 and 6 h post a single dose ($n = 4$ or 5 animals per group). Healthy groups are only shown for reference and were not included in statistical analysis. Data are shown as means ± SE, and comparisons made were DSS vs. DSS + WT_R2LC by two-way ANOVA multiple comparations followed by Dunnett's test (*B*, *H*) or Kruskal–Wallis test, followed by Dunn's multiple comparisons test (*D*, *E*, and *I*), $+P < 0.05$, and DSS vs. DSS + R2LC_CXCL12, $*P < 0.05$.

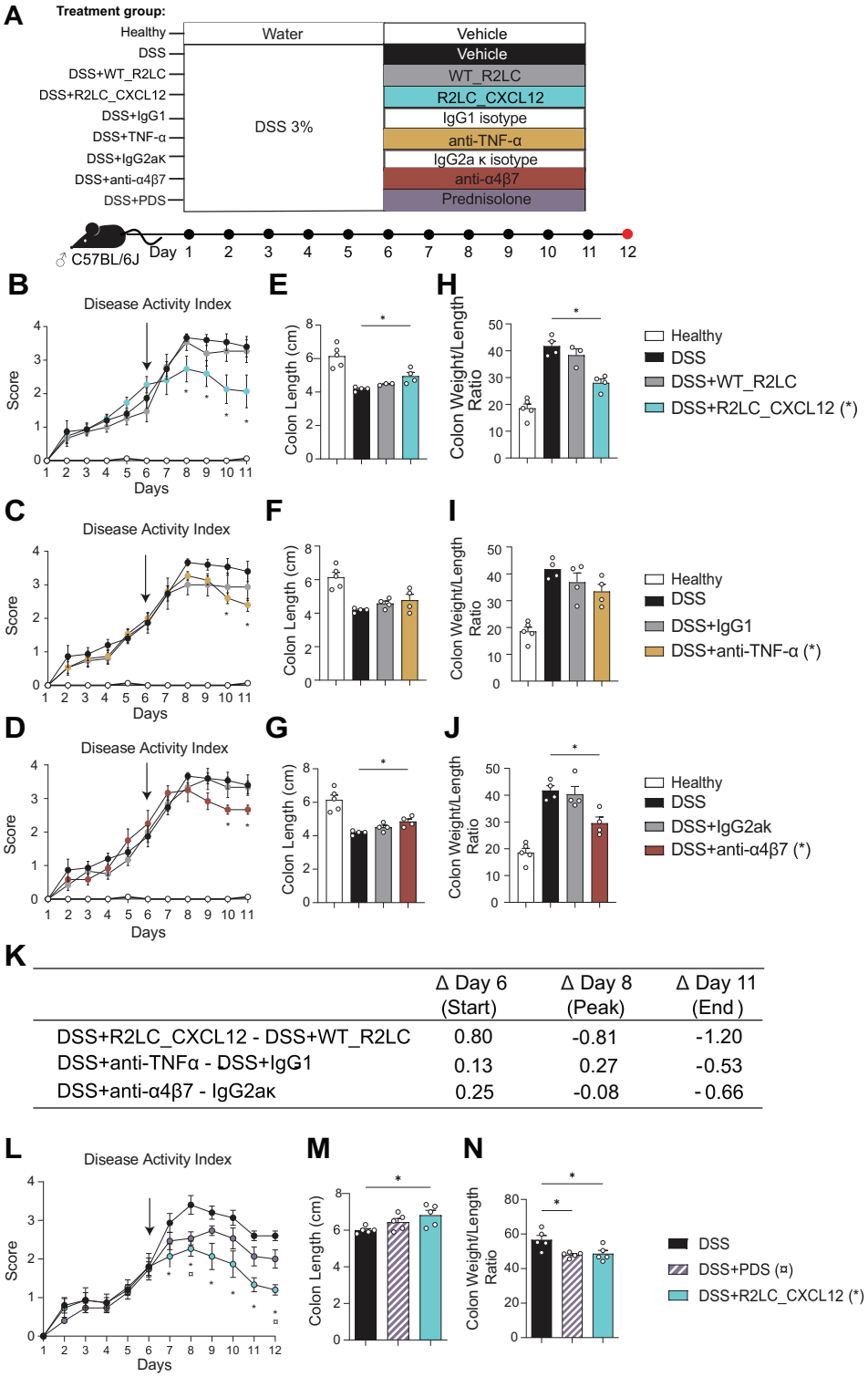

K

	Δ Day 6 (Start)	Δ Day 8 (Peak)	Δ Day 11 (End)
DSS+R2LC_CXCL12 - DSS+WT_R2LC	0.80	-0.81	-1.20
DSS+anti-TNFα - DSS+IgG1	0.13	0.27	-0.53
DSS+anti-α4β7 - IgG2aκ	0.25	-0.08	-0.66

Figure 2. R2LC_CXCL12 improves colitis more efficiently than anti-TNF-α, anti-α4β7, and steroid treatments. *A*: schematic overview of the experimental design to compare efficacies on colitis between R2LC_CXCL12 (100 μL per dose; 2×10^9 CFU per dose; three times a day) and current treatments in clinical use (5 mg/kg prednisolone, 250 μg/mouse anti-TNF-α, or 200 μg/mouse anti-α4β7, once a day). Disease activity index over time (arrow indicates start of treatment) (*B–D*), colon length (*E–G*), and colon weight-to-length ratio ($n = 4$ or 5 animals per group) (*H–J*) on *day 12* are presented. Data presented in *B–K* is from one independent experiment and healthy and dextran sulfate sodium (DSS) group are the same mice in *B–J*. *K*: delta disease activity index (DAI) for active treatments compared with their respective control on *day 6*, *day 8*, and *day 11*. DAI over time (arrow indicates start of treatment) (*L*), colon length (*M*), and colon weight-to-length ratio ($n = 5$ animals per group, one independent experiment) (*N*) on *day 12* are presented. Healthy groups are only shown for reference and were not included in statistical analysis. Data are shown as means ± SE, and comparisons made were DSS vs. DSS + R2LC_CXCL12, DSS vs. DSS + anti-TNF-α, DSS vs. DSS + anti-α4β7 by two-way ANOVA multiple comparations followed by Dunnett's test (*B–D*, *L*) or Kruskal–Wallis test, followed by Dunn's multiple comparisons test (*E–J*, *M–N*), $^*P < 0.05$, and DSS vs. DSS + prednisolone (PDS), $^\circ P < 0.05$.

Treatments

The mice were treated by gavage (100 μL) three times a day (unless stated otherwise) with suspensions of either vehicle (freezing solution), WT_R2LC, R2LC_murine CXCL12, or R2LC_human CXCL12, with treatment starting on *day 6*. The CXCL12 sequence of human and murine R2LC_CXCL12 only differs by one amino acid (29), and similar efficacies were observed. Thus, either treatment is referred to as R2LC_CXCL12 and was given at a dose of 2×10^9 CFU/dose in all experiments. Right before administration of bacterial solutions, the bacteria were activated by the addition of the SppIP peptide. The mice either received one dose before being euthanized, 2, 6, or 8 h postdose, or three doses a day

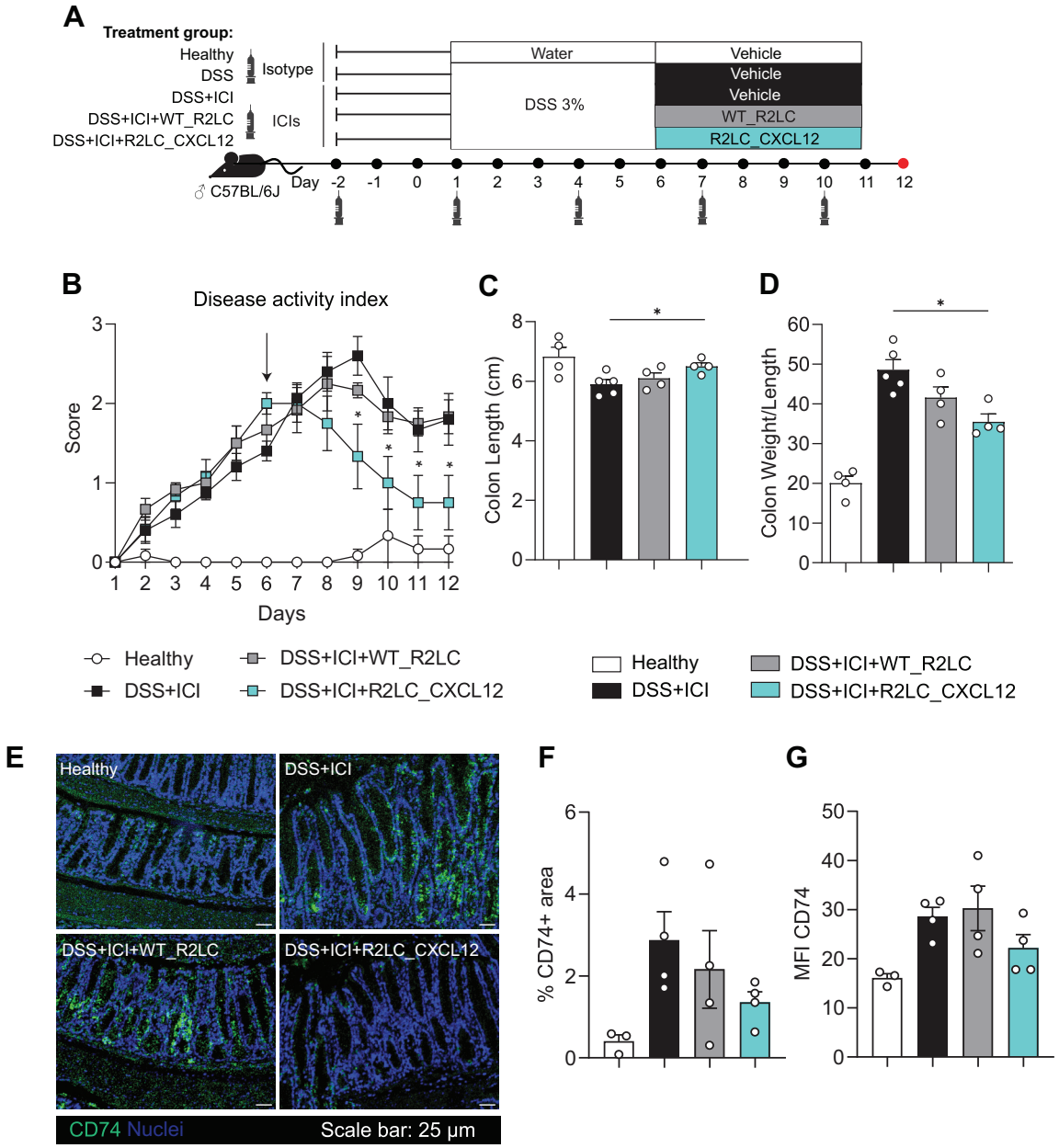

Figure 3. R2LC_CXCL12 ameliorates colitis symptoms in a mouse model of immune checkpoint inhibitor (ICI)-colitis. *A*: schematic overview of the experimental design of ICI-colitis where mice receiving both anti-PD-1 and anti-CTLA-4 (ICIs) treatment were challenged by dextran sulfate sodium (DSS). Anti-PD-1 and anti-CTLA-4, or their respective isotype controls (Isotype), were given on the days indicated with the syringe symbol. Red circle indicates the time point when mice were terminated. Disease activity index over time (arrow indicates start of treatment) (*B*), colon length (*C*), and colon weight-to-length ratio (*D*) on *day 12* ($n = 4$ or 5 animals per group, one independent experiment) are presented. Representative image of colonic tissue stained with CD74 (green) and DAPI (blue) (*E*), percentage (%) of CD74 + area (*F*), and CD74 mean fluorescence intensity (MFI) ($n = 4$ animals per group) (*G*) are presented. Healthy group was only included as a reference in the graph and was not part of the statistical test. Data are shown as means ± SE, and comparisons made were DSS + ICI vs. DSS + ICI + WT_R2LC, and DSS + ICI vs. DSS + ICI + R2LC_CXCL12 by two-way ANOVA multiple comparations followed by Dunnett's test (*B*) or Kruskal–Wallis test, followed by Dunn's multiple comparisons test (*C* and *D*, *F* and *G*), $^*P < 0.05$.

(at ~7–8 AM, 15–16 PM, 23–24 AM) for a total of 6 days. Rabbits were treated by oral administration of a capsule containing either control treatment or lyophilized R2LC_human CXCL12 together with the activation peptide SppIP.

Tissue Collection for Immunohistochemistry and Flow Cytometry

At the end of the experiments, the length and weight of the colons were recorded, and tissues [mesenteric lymph node (MLN), spleen, colon, small intestine, or ileum] were collected. Colon length and weight were used to assess colon shortening and the length-to-weight ratio, which is an indicator of inflammation and edema (30, 31). The tissues were analyzed using flow cytometry or histology.

Flow Cytometry

The expression of cell surface and intracellular markers on immune cells was determined by FACS analysis (BD LSR

Table 1. *Criteria for defining disease activity index score*

Score	Weight Loss	Stool Consistency	Intestinal Bleeding
0	None	Normal	Normal Occult negative
1	1–5%	Normal/loose	Slight bleeding detected Occult blood barely positive (±)
2	5–10%	Loose	Bleeding detected occult blood +
3	10–20%	Loose/diarrhea	Trace of bleeding detectable by eye in feces Occult + +.
4	>20%	Diarrhea	Rectal bleeding, gross bleeding

Fortessa, BD Biosciences) after surface staining or intracellular staining with specific antimouse antibodies. Cells were then stained using antibodies in Supplemental Table S1 to identify macrophages (CD45 + MHCII + CD64 + or CD45 + MHCII + F4/80 +), dendritic cells (DCs) (CD45 + MHCII + CD11c +), B cells (CD45 + CD19 +), innate lymphoid cells (ILCs) (CD45 + CD90 + CD3−), neutrophils (CD45 + CD11b + Ly6G +), monocytes (CD45 + CD11b + Ly6C +), T cells (CD45 + CD90 + CD3 +), IL-10 + cells, TGF-β (LAP) + cells, CXCL12 + cells, and CXCR4 + cells, as well as in combination for specific analysis.

Immunohistochemistry

Paraffin-embedded ileum Swiss roll sections were stained with primary antibodies anti-GL7 PE (1:300; 561530, BD PharMingen), anti-CXCR4^{total} (1:300, 53–9991-80, Thermo Fisher), and anti-CXCR4$^{non\text{-}P}$ (nonphosphorylated) (1:300, ab124824, Abcam) or control antibodies Rat IgM, K conjugated to PE (1:300, 400808, Biolegend), Rat IgG2b κ conjugated to Alexa Fluor 488 (1:300, 53–4031-80, Thermo Fisher), and rabbit monoclonal IgG (1:188, ab172730, Abcam). Paraffin-embedded colon Swiss roll sections were stained with anti-CD74 (1:100; ABIN7072640, Antibodies-Online), anti-MUC2 (1:500, ABIN2854828, Antibodies-online), anti-occludin (1:100, 71–1500, Abcam), IgG isotype (1:830, 910801, Biolegend), or IgG1 isotype control (1:70, 400432, Biolegend). For details, see Supplemental Methods.

Statistical Analysis

Data are presented as means ± SE, and analysis was performed using GraphPad Prism 9 (GraphPad Software, La Jolla, CA). The healthy groups have been included in the descriptive statistics for reference only. Outliers were identified using Grubb's test ($\alpha = 0.05$).

DAI were analyzed by two-way ANOVA multiple comparations followed by Dunnett's test. All data with more than two groups in the same time point were analyzed using Kruskal–Wallis test, followed by Dunn's multiple comparisons test (if the previous test $P < 0.05$).

RESULTS

Peroral Treatment with CXCL12-Expressing *Limosilactobacillus Reuteri* R2LC Ameliorates Colitis in Mice

The therapeutic potential of peroral administration of CXCL12-expressing *L. reuteri* R2LC (R2LC_CXCL12) was evaluated in mice where colitis was chemically induced by the addition of DSS to their drinking water. Of importance and in contrast to other models of colitis, DSS-induced colon inflammation develops in immune-competent mice, which is a prerequisite for the current study evaluating the efficacy of local immune modulation. During overt colitis (5 days following DSS onset), vehicle, wild-type R2LC (WT_R2LC), or R2LC_CXCL12 was administered by gavage three times daily (2×10^9 CFU/dose) (Fig. 1*A*). As a result, clinical symptoms (DAI score) were significantly improved 2 days after the first dose of R2LC_CXCL12 and continued to improve throughout the experiment, whereas no consistent improvement was observed following treatment with the wild-type bacteria (WT_R2LC) (Fig. 1, *B* and *C*). As a result, treatment with R2LC_CXCL12 prevented colon shortening when compared with vehicle treatment, as well as reduced colon weight-to-length ratio (Fig. 1, *D* and *E*), demonstrating less inflammation and edema formation.

To evaluate the intestinal presence and engraftment of R2LC_CXCL12 following peroral administration for 6 days, selective anaerobic culturing of fecal samples was performed using deMan, Rogosa, Sharpe (MRS) agar plates containing erythromycin and vancomycin. The samples were collected before treatment started (*day 6*), on the last day of treatment (*day 11*), and up to *day 24* or *72* in healthy and colitic mice (Fig. 1*F*). The *L. reuteri* R2LC identity and presence of the CXCL12-expressing plasmid were investigated by PCR of some of the R2LC-like (yellow) and non-R2LC-like (white) colonies (Supplemental Fig. S1, *A* and *B*). All tested R2LC-like colonies were confirmed to be R2LC_CXCL12, whereas the non-R2LC-like colonies were not *L. reuteri* R2LC and did not contain the CXCL12-expressing plasmids. Shortly after treatment, R2LC-like colonies were detected in feces from all R2LC_CXCL12-treated healthy mice (8 h after the last R2LC_CXCL12 dose, *day 11*, mean value $8.4 \times 10^4 \pm 4.7 \times 10^4$ CFU/g of feces), whereas a significant drop was observed 18 h after the last dose (*day 12*, $6.5 \times 10^3 \pm 2.2 \times 10^3$ CFU/g of feces) (Fig. 1*G*). In mice with DSS-induced colitis, R2LC-like colonies were detected in feces for a longer period following R2LC_CXCL12-treatment, even though they declined considerably in numbers when assessed at 19 days (*day 30*) or at later time points after the last dose (*day 24*: $1.3 \times 10^6 \pm 8.5 \times 10^5$ CFU/g of feces, less than 0.1% of the administered daily dose, *day 30*: $1.4 \times 10^5 \pm 6.0 \times 10^4$ CFU/g of feces, less than 0.01% of the daily dose). In some individuals, the R2LC-like colonies remained for a longer time point (3,000 CFU/g of feces at *day 37*, $n = 1$, and 500 CFU/g of feces at *day 58*, Fig. 1*G*). This observation likely reflects the inflammation-induced shift of the microbiota previously demonstrated (10). No colonies were detected after this time point, which demonstrates that R2LC_CXCL12-engraftment does not occur. Of interest, long-term DAI revealed that R2LC_CXCL12 treatment in colitic mice resulted in complete remission on *day 24*, which was nearly twice as fast as compared with the vehicle-treated mice (Fig. 1*H*) and coincided with the reduction of R2LC_CXCL12 in feces.

Exposure and translocation to tissues were evaluated at treatment start, after a completed cycle of treatment (three doses per day for 6 days) and when R2LC_CXCL12 was no longer detected in feces (Fig. 1*F*). As peroral R2LC has an intestinal transit time of 3 h in mice (32), exposure and translocation were investigated at 2 and 6 h postadministration to

allow for the highest probability of detection. However, R2LC_CXCL12 could not be detected in blood by selective culturing, and no changes in plasma levels of CXCL12 were observed at 2 or 6 h post single dose (Fig. 1*I*, Supplemental Table S2). Furthermore, selective culturing of blood samples and draining or highly perfused organs (liver, MLN, and spleen, respectively) collected after 6 days of treatment was performed, whereafter colonies were detected based on their R2LC-specific yellow color and characteristics and referred to as R2LC-like. Although no translocation of R2LC could be detected in circulation or spleen (Supplemental Table S3), R2LC-like colonies were detected in the liver of colitic mice (DSS + WT_R2LC: 5/14 mice and DSS + R2LC_CXCL12− mice: 10/14 mice), which was expected considering the portal drainage from the GI tract. Selective culturing of MLNs also revealed R2LC-like colonies in colitic mice treated with R2LC_CXCL12 (3/5) but not WT_R2LC (Supplemental Table S3). However, in mice with DSS-induced colitis, no R2LC_CXCL12 could be detected in blood, spleen, kidneys, liver, or lungs at *day 72* (61 days post last R2LC_CXCL12 dose) (Supplemental Table S4). These results confirm that peroral treatment with R2LC_CXCL12 does not result in systemic exposure and that the bacteria do not translocate to the tissues and remain in the GI tract only until amelioration of colitis.

R2LC_CXCL12 Induces Stronger and Faster Resolution of Symptoms than Approved Biologics

The efficacy of R2LC_CXCL12 treatment in ameliorating colitis was benchmarked in a head-to-head study, where the anti-TNF-α and anti-α4β7 demonstrating the highest potency in mice were selected (Fig. 2*A*). In agreement with the results presented in Fig. 1*B*, R2LC_CXCL12-treated mice showed consistent improvement of DAI score after 2 days of treatment (*day 8* and beyond, Fig. 2*B*), whereas anti-TNF-α and anti-α4β7 treatments improved DAI score after 4 days (from *day 10*, Fig. 2, *C* and *D*). No improvement was observed in mice receiving the corresponding control treatments: WT_R2LC, IgG1 isotype, or IgG2aκ isotype (Fig. 2, *B*–*D*). Treatment with R2LC_CXCL12 and anti-α4β7, but not anti-TNF-α, reduced the colon shortening and the colon weight-to-length ratio compared with vehicle-treated mice (Fig. 2, *E*–*J*), demonstrating reduced inflammation and edema formation of the two former therapies. Furthermore, R2LC_CXCL12 had reduced mean DAI by −1.20 compared with control treatment (WT_R2LC) at the end of treatment, which is almost twice the effect size as for anti-TNF-α and anti-α4β7 when compared with their respective matched control treatments (IgG1 and IgG2aκ) (Fig. 2*K*, Supplemental Table S5). Of importance, these differences were observed even though the mean DAI at the start of treatment was highest for the group receiving R2LC_CXCL12 (*day 6*). When compared with the corticosteroid prednisolone (PDS), the currently most common first line of treatment for IBD and ICI-colitis, R2LC_CXCL12-treated mice showed a consistent improvement in DAI score after 2 days of treatment (from *day 8*, Fig. 2*L*), whereas PDS only transiently improved DAI after 2 days and at the end of the experiment (Fig. 2*A*). In addition, only R2LC_CXCL12 showed reduced colon shortening (Fig. 2*M*), whereas both treatments showed a reduction in ratio of colon weight to length (Fig. 2*N*). Together, these data demonstrate that R2LC_CXCL12 efficiently ameliorates DSS-induced colitis in mice and that resolution of symptoms in response to R2LC_CXCL12 occurs faster when compared with approved biologic therapies and the current first line of treatment.

R2LC_CXCL12 Ameliorates Colitis in Mice on ICI Treatment

Although colitis is a common side effect of ICI therapies in humans, this is not observed to the same extent in mice (33, 34). To evaluate if R2LC_CXCL12 treatment would also be beneficial for ICI-colitis, mice were treated with a combination of anti-PD-1 and anti-CTLA-4 before and during DSS-induced colitis (Fig. 3*A*). This protocol resulted in DAI similar to DSS-induced colitis (Supplemental Fig. S2, *A*–*C*), whereas the levels of mucosal CD74, known to be upregulated in colitis (35) were increased and therefore indicates aggravated mucosal inflammation by the combination therapy (Supplemental Fig. S2, *D*–*E*). Treatment with R2LC_CXCL12 in mice with overt ICI-DSS colitis resulted in an improved DAI score after 3 days (from *day 9*, Fig. 3*B*), whereas the wild-type bacteria had no therapeutic effect. In addition, R2LC_CXCL12 treatment resulted in reduced colon shortening and reduced colon weight-to-length ratio when compared with DSS-ICI mice treated with vehicle (Fig. 3, *C* and *D*), demonstrating reduced inflammation and edema formation. Furthermore, the $CD74^+$ area in the mucosal tissue shows a tendency toward reduction in R2LC_CXCL12-treated animals (Fig. 3, *E*–*G*). Thus, these results suggest that treatment with R2LC_CXCL12 also ameliorates colitis in mice on ICI treatment.

In another set of experiments, 4T1 breast tumor-bearing BALB/c mice received anti-PD-1 treatment for 3 wk, whereafter changes in colon length as well as erosions and ulcers in the colonic epithelia could be detected (Supplemental Fig. S3*A*). Of interest, in the group receiving oral treatment with R2LC_CXCL12 for the last week, fewer erosions and ulcers were detected in the colon of the tumor-bearing mice (Supplemental Fig. S3, *B*–*C*). None of the treatments had any effect on tumor size (Supplemental Fig. S3*D*) but indicates local promotion of mucosal healing following peroral R2LC_CXCL12.

Limosilactobacillus Reuteri R2LC-Delivered CXCL12 Induces Transient CXCR4 Signaling in Immune Cells in PPs

To determine the site of action of the bacteria-delivered CXCL12, ileum was collected at 8 h following oral gavage of either vehicle, WT_R2LC, or R2LC_CXCL12 to mice with DSS-induced colitis. Using immunohistochemistry, intracellular and surface levels of CXCR4 ($CXCR4^{total}$), as well as nonphosphorylated CXCR4 ($CXCR4^{non\text{-}P}$) were analyzed (Fig. 4*A*), as CXCR4 undergoes COOH-terminal phosphorylation upon binding of CXCL12 and reduced $CXCR4^{non\text{-}P}$ therefore indicates ligand binding and activation (36). In the ileal mucosa as well as in the PPs, the $CXCR4^{total}$ signal was distributed throughout the cytoplasm and cell surface. In contrast, the $CXCR4^{non\text{-}P}$ signal was distributed in a more speckled pattern (Fig. 4*A*), which previously has been reported to occur in response to CXCL12 signaling (37). CXCL12 is known to be abundantly expressed in the PPs, predominantly in the dark

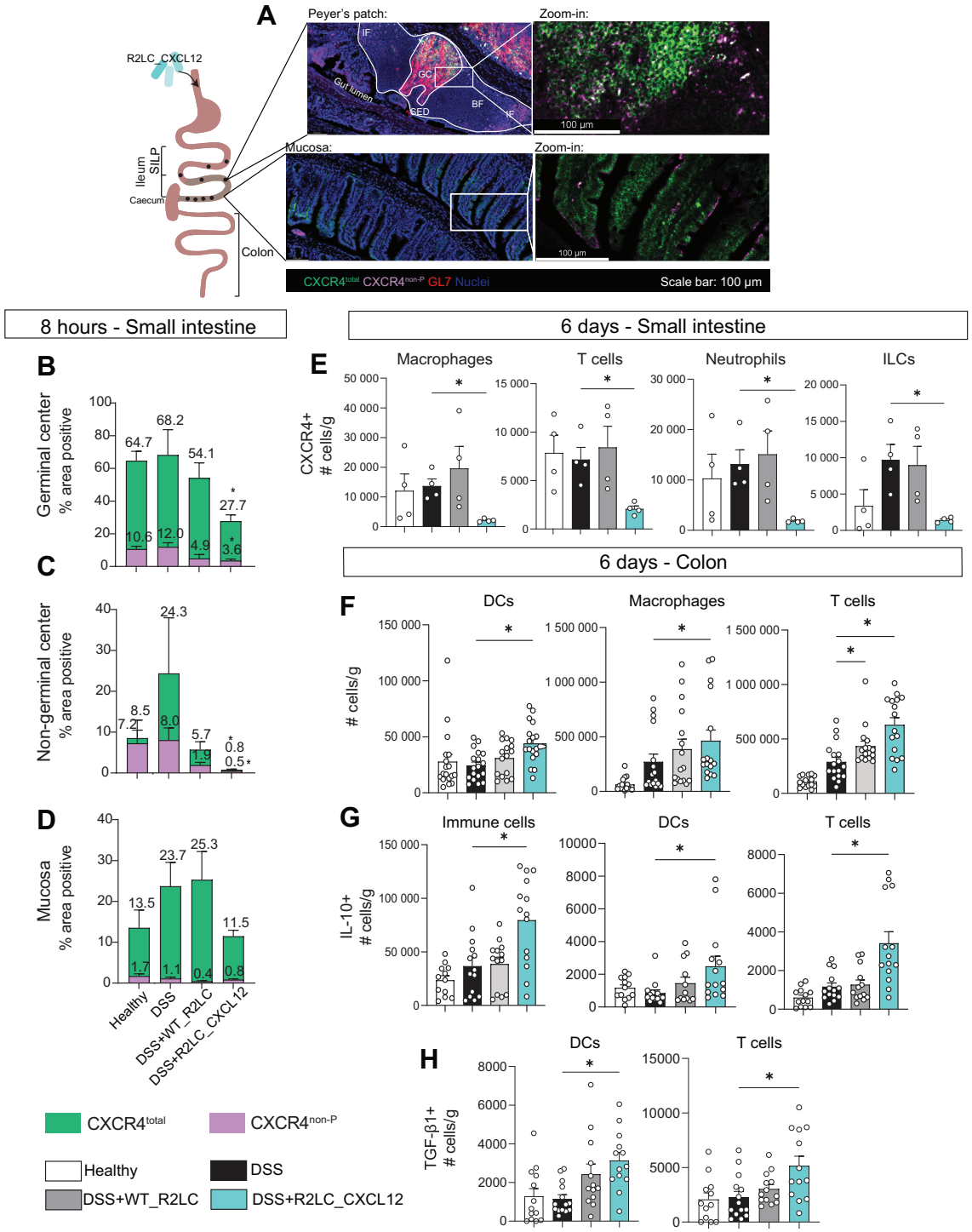

Figure 4. Oral administration of R2LC_CXCL12 induces CXCR4 signaling in Peyer's patches, reduces surface expression of CXCR4 in small intestinal immune cells, and induces tolerogenic immune cell subsets in colon. *A*: representative immunofluorescent image of nuclei (blue), GL7 (red), $CXCR4^{total}$ (green), and $CXCR4^{non\text{-}P}$ (magenta) staining in the Peyer's patches (PPs) and ileal mucosa of mice with dextran sulfate sodium (DSS)-induced colitis 8 h after administration of vehicle. GL7 signal marks the germinal center (GC) of the B-cell follicles (BFs) in PPs. B-cell follicles (BFs) are separated by less dense T-cell-rich interfollicular regions (IFs) and include the subepithelial dome (SED) covered in follicle-associated epithelium facing the gut lumen. Areas positive for $CXCR4^{total}$ (green) and $CXCR4^{non\text{-}P}$ (magenta) in the PPs ($n = 3$ or 4 animals per group (*B* and *C*) and ileal mucosa ($n = 3$ or 4 animals per group, one independent experiment) (*D*) at 8 h after administration are presented. *E*: number of $CXCR4^{+}$ macrophages, T cells, neutrophils, and ILCs in the small intestine lamina propria in healthy mice treated with vehicle, and mice with DSS-induced colitis treated with vehicle, WT_R2LC, or R2LC_CXCL12 for 6 days ($n =$ 4 animals per group). Number of DCs, macrophages, and T cells in colonic lamina propria (*F*), number of $IL\text{-}10^{+}$ immune cells, DCs, and T cells (*G*), and number of $TGF\text{-}\beta1^{+}$ DCs and T cells (*H*) in the colonic lamina propria in healthy mice treated with vehicle and mice with DSS-induced colitis treated with vehicle, WT_R2LC, or R2LC_CXCL12 for 6 days, three doses per day ($n = 12$–14 animals per group, four independent experiments) are shown. Healthy group is only shown for reference and was not included in statistical analysis. Data are shown as means ± SE, and comparisons made were DSS vs. DSS + WT_R2LC and DSS vs. DSS + R2LC_CXCL12 by Kruskal–Wallis test, followed by Dunn's multiple comparisons test (*B*–*H*), $*P < 0.05$.

zone of the germinal center (GC) (38–41). Distinct CXCR4$^+$ and CXCR4$^-$ regions could be detected within the GC of the PPs, and to a much lower extent in the non-GC part (including the subepithelial dome and interfollicular zone) (Fig. 4*A*). At 8 h following treatment with R2LC_CXCL12 but not WT_R2LC in colitic mice, the areas positive for CXCR4$^{non\text{-}P}$ and CXCR4^{total} were significantly reduced (both GC and non-GC) when compared with vehicle treatment (Fig. 4, *B* and *C*). This suggests phosphorylation (reduced CXCR4$^{non\text{-}P}$) and degradation of CXCR4 (decrease of CXCR4^{total}) at 8 h. Long-term exposure to CXCL12 (overnight) has been reported to result in degradation of the CXCR4 receptor (36), and the altered CXCR4 levels in the PPs following R2LC_CXCL12 treatment demonstrate delivery of the bacterial-produced CXCL12 to this site. In the mucosa (epithelium and lamina propria), the levels of CXCR4$^{non\text{-}P}$ were low irrespective of treatment, and a trend toward reduction in CXCR4^{total} levels could be detected following treatment with R2LC_CXCL12 compared with vehicle (Fig. 4*D*). In summary, these results indicate that oral administration of a single dose of R2LC_CXCL12 activates CXCR4$^+$ cells predominantly in the PPs.

To understand the effect of multiple-dose treatment with R2LC_CXCL12 on CXCR4 expression in the small intestine, flow cytometric analysis of lamina propria immune cells was carried out after 6 days of daily treatment of healthy and colitic mice (gating strategies: Supplemental Figs. S4, S5, and S6). Although no changes were observed in total immune cell count, R2LC_CXCL12-treated mice had a tendency toward a reduced number of immune cells expressing CXCR4 on the cell surface (Supplemental Fig. S7*A*). A more detailed analysis of the different immune cell subpopulations in the small intestinal lamina propria (SILP) following R2LC_CXCL12-treatment in colitic mice revealed a reduction of neutrophils and macrophages to similar levels as observed in healthy mice, as well as of CXCR4$^+$ macrophages, T cells, neutrophils, and ILCs (Fig. 4*E*, Supplemental Fig. S7*B*). No reduction was observed for dendritic cells (DCs), T cells, B cells, monocytes, or innate lymphoid cells (ILCs), nor for CXCR4$^+$ DCs and monocytes. In addition, no effects were detected on IL-10$^+$, TGF-β (LAP)$^+$, or CXCL12$^+$ immune cell counts at this site (Supplemental Fig. S7*C*). Of importance, no effects on the number of immune cells, immune cell subpopulations, or their respective expression of surface CXCR4 or total CXCL12 were observed in MLN and spleen (Supplemental Fig. S8, *A*–*D*), which supports a restricted local immune effect induced by the R2LC_CXCL12 treatment and that a site of interaction is located within the small intestine. Together, these results demonstrate that orally administered R2LC_CXCL12 delivers the CXCL12 mainly at PPs in the ileum in a true local manner, as no effects were observed on CXCR4 or CXCL12 cells in secondary lymphoid organs.

R2LC_CXCL12 Treatment Induces an Anti-Inflammatory Phenotype of Immune Cells in the Colonic Lamina Propria

To further investigate the mechanism of action by which colitis is ameliorated by R2LC_CXCL12 treatment, analysis of immune cells in the colon was performed after 6 days of treatment (2×10^9 CFU, three times a day). These experiments revealed a trend toward increased immune cell numbers by WT_R2LC and R2LC_CXCL12 when compared with vehicle (Supplemental Fig. S9*A*). Specifically, the numbers of DCs, macrophages, and T lymphocytes were significantly increased by the R2LC_CXCL12 treatment, whereas WT_R2LC increased only the T-cell population (Fig. 4*F*, Supplemental Fig. S5). No differences were found in the total number of B cells, monocytes, neutrophils, or ILCs irrespective of treatment (Supplemental Figs. S5 and S9*A*). Phenotype profiling revealed a significant increase in the number of immune cells expressing IL-10 following R2LC_CXCL12 but not WT-R2LC-treatment in mice with overt colitis, which was due to increased expression of IL-10 in DCs and T lymphocytes (Fig. 4*G*). In addition, TGF-β1 expression was increased in DCs and T lymphocytes by R2LC_CXCL12 treatment in colitic mice (Fig. 4*H*, Supplemental Fig. S6), even though it was not significantly elevated in the general immune cell population (Supplemental Fig. S9*B*). No treatment-related differences were observed for CXCR4$^+$ or CXCL12$^+$ cells in the colonic lamina propria (Supplemental Figs. S4 and S9, *B*–*C*), confirming that bacterial-derived CXCL12 is mainly inducing CXCR4 signaling at the PPs in the ileum and not in the colon. In addition, the previous observation of *L. reuteri* R2LC-induction of IgA (10) was also confirmed by R2LC_CXCL12 treatment. Thus, an increased proportion of IgA+ bacteria and IgA mean fluorescence intensity (MFI) were observed in the outer colonic mucus levels as a consequence of WT_R2LC and R2LC_CXCL12 treatment in healthy mice, whereas free IgA levels in the colonic mucus were increased in WT_R2LC-treated animals (Supplemental Fig. S10, *A*–*D*). These results reveal that R2LC_CXCL12 treatment in mice with overt colitis induces increased numbers of anti-inflammatory, immunoregulating DCs and T cells in the colon mucosa, as well as increased levels of IgA. Treatment with wild-type R2LC in healthy mice has previously been shown to upregulate tight junction proteins, including ZO-1 and occludin in the colon epithelia, as well as increase mucus thickness (11). In the current study, the expression of occludin and Muc2 was assessed at the end of experiments using immunohistochemistry of the entire colon tissues. A decrease in occludin expression was observed apically in the colonic crypts in mice with DSS-induced colitis compared with healthy mice, whereas no difference in MUC2 or occludin was observed between treatment groups (Supplemental Fig. S11, *A*–*F*).

Multidose Administration of ILP100 Oral to Rabbits Confirm Product Feasibility and Tolerability

The R2LC_CXCL12 was formulated as a lyophilized powder and was, together with the lyophilized activation peptide SppIP, filled in capsules designed to dissolve in neutral pH to deliver the contents in the small intestine, designated as ILP100 Oral. Intact bioactivity of CXCL12 derived from the freeze-dried *L. reuteri* R2LC was demonstrated in vitro using a β-arrestin cell-based assay (Supplemental Fig. S12). Three different doses of ILP100 Oral were manufactured and confirmed by viable cell count: 10^8 CFU (low dose),10^9 CFU (medium dose), and 10^{10} CFU (high dose). To assess safety and

tolerability, healthy New Zealand rabbits received daily dosing for 4 wk of either placebo or ILP100 Oral of low or medium dose (Fig. 5*A*), which did not result in any differences in daily food intake, body weight, clinical signs, or ophthalmoscopy. Furthermore, no treatment-related findings in hematology, coagulation, clinical chemistry, or urinalysis were detected either pretreatment or at the end of the study on *day 29/30* (specification of assessments in Supplemental Tables S6, S7, and S8). Furthermore, no findings were reported in the histopathology analyses carried out at the end of the study for all tissues and organs in any sample for any group (specification of assessments in Supplemental Table S9). In addition, there were no differences in plasma levels of CXCL12 between groups at any time point (Fig. 5*B*), and no R2LC_CXCL12 colonies were detected by selective culturing of blood at any of the time points (Supplemental Table S10). Finally, biodistribution was assessed following three doses of either placebo or ILP100 Oral high (at *day 1*) to healthy New Zealand rabbits, whereafter exposure to blood, kidneys, lungs, or spleen was evaluated at *day 3* (Fig. 5*C*). No colonies were detected in any of the samples in any of the treatment groups (Fig. 5*D*). These results confirm that administration in capsules with the lyophilized formulation is feasible and well tolerated for delivery of the ILP100 Oral to the gastrointestinal tract with no systemic detectable exposure.

DISCUSSION

Current therapies targeting colitis rely on dampening inflammation by suppressing the immune system and are associated with systemic adverse effects, including increased susceptibility to infections. In the current study, means to locally stimulate the intestinal immune system to heal mucosal injuries without inducing systemic immune effects were investigated in different models of colitis. We found that oral administration of *L. reuteri* R2LC engineered to express CXCL12 (R2LC_CXCL12) (42) ameliorated overt DSS-induced and DSS-ICI-induced colitis through local immunoregulatory actions induced in the PPs. As a result, the numbers of IL-10- and TGF-β1-producing cells increased in the colon lamina propria, and clinical symptoms were reduced. Of importance, no systemic effects on immune cells could be found, and no R2LC bacteria or elevated levels of CXCL12 were detected in circulation, spleen, or lungs, but R2LC were found in the liver and MLN directly following administration to diseased mice. Furthermore, the efficacy of the R2LC_CXCL12 treatment on clinical symptoms was superior when benchmarked to current treatments of choice, anti-TNF-α, anti-α4β7, and corticosteroids. Finally, therapeutic feasibility was proven as lyophilized bacteria produced CXCL12 with maintained bioactivity, and capsules with lyophilized bacteria and the activation peptide were well tolerated, whereas no systemic effects were demonstrated in rabbits following peroral treatment.

The involvement of intestinal microbiota in gastrointestinal health is increasingly recognized, and several studies demonstrate associations between distinct bacterial strains and clinical symptoms in animal models of colitis and in patients (1–8). However, the importance of the microbiota composition, site of interactions between the bacteria and the host immune cells, as well as the consecutive downstream host mechanisms have not yet been clarified. We have previously found that wild-type *L. reuteri* R2LC prevents the development of colitis when given prophylactically

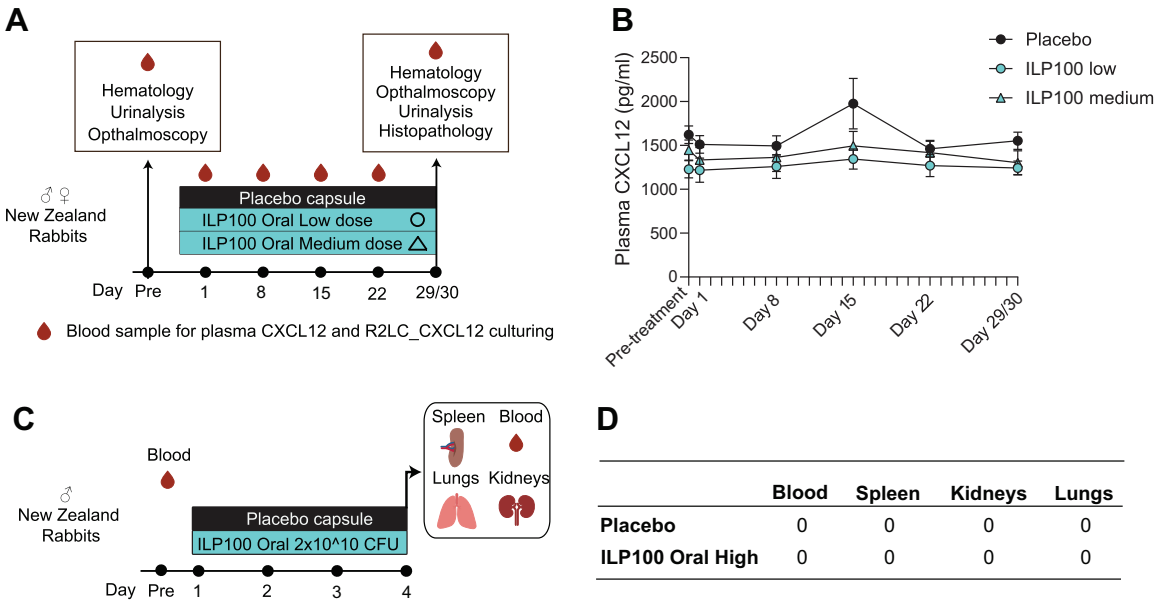

	Blood	Spleen	Kidneys	Lungs
Placebo	0	0	0	0
ILP100 Oral High	0	0	0	0

Figure 5. Summary of product feasibility and tolerability studies of ILP100 Oral in New Zealand rabbits. *A*: schematic overview of the experimental design for a 4-wk multidose study in New Zealand rabbits. *B*: plasma CXCL12 levels of placebo, ILP100 Oral (low), and ILP100 Oral (medium) rabbits ($n = 6$ animals per group, one independent experiment). *C*: schematic overview of the experimental design of biodistribution study in New Zealand rabbits ($n = 3$ animals per group, one independent experiment). *D*: number of colonies in blood, spleen, kidneys, and lungs ($n = 3$ animals, $N = 6$ culture plates per group). Data are shown as means ± SE, and comparisons made were placebo vs. ILP100 Oral low_R2LC and vs. ILP100 Oral medium by two-way ANOVA multiple comparations followed by Dunnett's test (*B*).

before DSS induction of colitis (10, 11). *L. reuteri* is a common, nonpathogenic, Gram-positive bacterial organism found naturally in the gut of humans and other warm-blooded animals and has a history as a food additive to improve mouth and gut health (43, 44). Recently, we revealed that the mechanism by which *L. reuteri* R2LC conveys the anti-inflammatory effects in the gut involved enhanced induction of IgA in B lymphocytes at the PPs, followed by increased trafficking of IgA-producing B lymphocytes to the ileal and colonic mucosa and concomitant augmented IgA levels in the gut lumen. As a consequence, the gut microbiota shifted toward more health-associated, and clinical symptoms during DSS-induced colitis were significantly improved (10). In contrast, when administered during overt colitis, no treatment effect of WT_R2LC could be detected in the current study. PPs are the most intense site of IgA induction in the entire body, and they thereby regulate the intestinal microbiota and are important for preventing the growth of pathogenic microbes (9). Of interest, the CXCR4/CXCL12 axis is critical for proper cell trafficking and the production of antibody-producing plasma B lymphocytes within PPs (39–41). When R2LC_CXCL12 was administered to mice with overt DSS-induced colitis in the current study, the clinical symptoms were significantly ameliorated in parallel with reduced numbers of distinct $CXCR4^+$ immune cell populations in the small intestine and increased populations of immuneregulatory, tissue-healing immune cells in the colon. Of importance, no changes were observed on CXCR4 or CXCL12 levels in the secondary lymphoid organ spleen and MLN nor in the colon, demonstrating that the site of action of bacteria-produced CXCL12 is exerting its effects in the small intestine. Furthermore, the previously reported R2LC-dependent induction of IgA resulting in increased colonic IgA levels (10) was also confirmed by the R2LC_CXCL12 treatment. Tissue restorative and anti-inflammatory actions of oral administration of R2LC_CXCL12 were demonstrated in the colon of colitic mice, as the number of TGF-$\beta1^+$ and IL-10^+ dendritic cells and T cells were increased after 6 days of treatment when compared with vehicle-treated mice. Both of these cytokines are known to be major suppressors of intestinal inflammation (45–47).

To be relevant as interventional therapy for colitis, safety and efficacy profiles need to be competitive and offer added value and a new pathway should be provided for patients not responding to current treatments. Today, patients with IBD are treated with systemic corticosteroids and biologics, including, for example, anti-TNF-α and anti-$\alpha4\beta7$, as well as JAK inhibitors. When treating these chronic diseases, rotation of biologics is often done as resistance to therapy develops and the effect is lost due to the development of anti-drug antibodies (ADAs). This is reflected by the large total market size of the approved biologics and the vast pipeline compared with the number of eligible patients with UC. Local-acting alternatives to the above-mentioned systemically acting biologics should provide a more acceptable safety profile and less risk of ADA development, and thereby reduce the proportion of patients becoming refractory nonresponders. Drug candidates aiming for local-acting effects that are or have been investigated for therapeutic efficacy include the peptide melanocortin receptor agonist PL-8177, administered orally, where resolution of inflammation was reported, together with adverse events such as abdominal pain, nausea, and vomiting, and dizziness already at subclinical levels of dosing (48). Furthermore, the S1P modulator Zeposia has been repurposed and approved for UC, and another S1P1 agonist is currently being investigated [APD334/Etrasimod (NCT02447302)] (48, 49). Local targeting of TLR9 (e.g., Cobitolimod) is evaluated in late-stage clinical development (NCT04985968). Furthermore, as a natural development of clinical fecal transplantations, a number of drug candidates aim to change the microbiota in patients with UC using consortia-type products such as VE202 and SER-287.

The use of bacteria as vectors to deliver recombinant therapeutic proteins is emerging, as this approach allows for a continuous and local production of short-lived proteins and peptides (50, 51). There are currently at least three types of drug candidates in clinical development, and the research pipeline is expanding to include multiple species and strains of bacteria, proteins, and RNA delivered through different routes of administration. *Lactococcus lactis* delivering recombinant IL-10 (AG011) to the intestine of patients with UC has been evaluated in clinical trials, but no efficacy was reported, and the programs were discontinued (NCT00729872). The engineered bacteria of the current study (ILP100) have previously been demonstrated to increase healing of induced cutaneous wounds following topical delivery in mice, pigs, as well as in a first-in-human study designed to primarily assess safety and tolerability (29, 52, 53). In these studies, the chemokine CXCL12 is locally delivered to induced skin wounds, which results in accelerated healing through an increased population of TGF-β-expressing macrophages at the wound edge. Of importance, the levels of systemic CXCL12 in plasma were not increased by the treatment, and no difference in tissue levels at 48 h following a single dose administration was detected by ELISA. However, an increase in $CXCL12^+$ cells was detected in the ILP100-treated skin wounds at 48 h posttreatment. Together with no systemic detection or skin colonization of the administered, engineered bacteria, topical treatment of ILP100 was considered both safe and tolerable, as well as revealed biological effect on healing, and clinical development is now further warranted in patients.

Although immune checkpoint inhibition offers a novel strategy to treat cancer, it also causes serious immune-related adverse effects, of which those affecting the GI tract (e.g., ICI-induced colitis) are among the most common in patients receiving dual anti-CTLA-4 and anti-PD-1 therapy. These adverse effects often necessitate dose reduction or discontinuation of anticancer treatment altogether (54, 55). Although there may be overlapping features of UC and ICI-induced colitis, it is important to recognize that distinct differences are actively being identified and delineated. Despite these differences, ICI-colitis is currently treated with therapeutics developed for UC, including immunosuppressive steroids, anti-TNF-α, and anti-$\alpha4\beta7$, which all act systemically and can reduce the antitumor efficacy of the ICIs (54). Experimental, short-term mouse studies suggest that anti-TNF-α helps against anti-PD-1 resistance in melanoma and reduces ICI-induced toxicities if given

prophylactically; however, this has not yet been reported in clinical prospective studies (33, 56). Thus, the need for local-acting anti-inflammatory new treatments is currently most pronounced in ICI-induced colitis. In the current study, colitis was not aggravated by the immune checkpoint inhibitors when assessed by macroscopic disease activity measurements, as previously described (33). However, histopathological changes were confirmed, suggesting that the local environment in the colon tissue is altered by the ICI therapy during DSS treatment. Of importance, R2LC_CXCL12 also improved DAI in mice with DSS- and ICI-induced colitis, demonstrating the feasibility of therapeutic R2LC_CXCL12 to ameliorate colitis also during ICI therapy.

The limitations of the current study include those associated with the experimental models of DSS- and ICI-induced colitis and their relevance for human disease, as well as the relevance of the investigated bacterial strain in humans. However, mechanistic therapeutic insights are important to acquire from in vivo studies of experimental models but certainly require confirmation in humans and patients during clinical development. As first steps toward translation of the drug candidate, we developed capsules containing lyophilized R2LC_CXCL12 and activation peptide, SppIP, whereafter maintained bacterial viability and activity of the bacteria-produced chemokine were demonstrated. Furthermore, two safety studies in rabbits reported no systemic distribution of bacteria or altered levels of plasma CXCL12, similar to the findings in mice and in line with the previous reported data from the development of the ILP100-Topical (52, 53). These results provide evidence for feasibility and low-risk profile of the formulated drug product, ILP100 Oral, for continued developments in a first-in-human clinical trial.

In summary, this study reports that therapeutic oral administration of R2LC_CXCL12 effectively ameliorates colitis in two experimental mouse models through local effects on the intestine, as the bacteria deliver CXCL12 to the PPs and shift the colonic immune cell profile toward tolerogenic phenotypes. Furthermore, both feasibility and low-risk profile of the formulated ILP100 Oral were demonstrated in rabbits and together with the efficacy data support a competitive positioning of the ILP100 Oral for clinical development as an interventional therapy in colitis.

DATA AVAILABILITY

The data presented in this study are available on request from the corresponding author.

SUPPLEMENTAL DATA

Supplemental Figs. S1–S12 and Supplemental Tables S1–S10: https://doi.org/10.6084/m9.figshare.25699155.v1.

GRANTS

This study was supported by Ilya Pharma AB, a BioX grant from STUNS to Ilya Pharma AB, and by the Swedish Research Council, Knut and Alice Wallenberg Foundation (to M. Phillipson).

DISCLOSURES

M.P., S.R., M.J., P.F., and EV are shareholders of Ilya Pharma. E.V., E.Ö., H.L.T., Y.P., C.D., and M.C.L. have stocks options in Ilya Pharma. E.Ö., E.V., H.L.T., P.F., K.P., and Y.P., were or are employees, part time or full time, of Ilya Pharma AB. M.J. is consultant paid by Ilya Pharma AB for their services. M.P. receives renumeration for work in the company Board of Directors. None of the other authors has any conflicts of interest, financial or otherwise, to disclose.

AUTHOR CONTRIBUTIONS

E.Ö., K.P., J.C., M.O., P.F., E.V., and M.P. conceived and designed research; E.Ö., C.D., Y.P., M.C.L, V.R.G., J.C., and M.O. performed experiments; E.Ö., C.D., K.P., Y.P., H.L.T., M.C.L., V.R.G, and E.V. analyzed data; E.Ö., C.D., K.P., H.L.T., and E.V. interpreted results of experiments; E.Ö. and K.P. prepared figures; E.Ö., C.D., and K.P. drafted manuscript; E.Ö., K.P., M.J., S.R., E.V., and M.P. edited and revised manuscript; E.Ö., C.D., K.P., Y.P., H.L.T., M.C.L., V.R.G., J.C., M.O., P.F., M.J., S.R., E.V., and M.P approved final version of manuscript.

REFERENCES

1. **Gopalakrishnan V**, **Helmink BA**, **Spencer CN**, **Reuben A**, **Wargo JA.** The influence of the gut microbiome on cancer, immunity, and cancer immunotherapy. *Cancer Cell* 33: 570–580, 2018. doi:10.1016/j.ccell.2018.03.015.
2. **Schnupf P**, **Gaboriau-Routhiau V**, **Cerf-Bensussan N.** Modulation of the gut microbiota to improve innate resistance. *Curr Opin Immunol* 54: 137–144, 2018. doi:10.1016/j.coi.2018.08.003.
3. **Wang T**, **Zheng N**, **Luo Q**, **Jiang L**, **He B**, **Yuan X**, **Shen L.** Probiotics Lactobacillus reuteri abrogates immune checkpoint blockade-associated colitis by inhibiting group 3 innate lymphoid cells. *Front Immunol* 10: 1235, 2019. doi:10.3389/fimmu.2019.01235.
4. **Schroeder BO**, **Bäckhed F.** Signals from the gut microbiota to distant organs in physiology and disease. *Nat Med* 22: 1079–1089, 2016. doi:10.1038/nm.4185.
5. **Wu H**, **Tremaroli V**, **Schmidt C**, **Lundqvist A**, **Olsson LM**, **Krämer M**, **Gummesson A**, **Perkins R**, **Bergström G**, **Bäckhed F.** The gut microbiota in prediabetes and diabetes: a population-based cross-sectional study. *Cell Metab* 32: 379–390.e3, 2020. doi:10.1016/j.cmet.2020.06.011.
6. **Qin J**, **Li Y**, **Cai Z**, **Li S**, **Zhu J**, **Zhang F**, **et al.** A metagenome-wide association study of gut microbiota in type 2 diabetes. *Nature* 490: 55–60, 2012. doi:10.1038/nature11450.
7. **Fu J**, **Bonder MJ**, **Cenit MC**, **Tigchelaar EF**, **Maatman A**, **Dekens JAM**, **Brandsma E**, **Marczynska J**, **Imhann F**, **Weersma RK**, **Franke L**, **Poon TW**, **Xavier RJ**, **Gevers D**, **Hofker MH**, **Wijmenga C**, **Zhernakova A.** The gut microbiome contributes to a substantial proportion of the variation in blood lipids. *Circ Res* 117: 817–824, 2015. doi:10.1161/CIRCRESAHA.115.306807.
8. **Sokol H**, **Pigneur B**, **Watterlot L**, **Lakhdari O**, **Bermúdez-Humarán LG**, **Gratadoux J-J**, **Blugeon S**, **Bridonneau C**, **Furet J-P**, **Corthier G**, **Grangette C**, **Vasquez N**, **Pochart P**, **Trugnan G**, **Thomas G**, **Blottière HM**, **Doré J**, **Marteau P**, **Seksik P**, **Langella P.** Faecalibacterium prausnitzii is an anti-inflammatory commensal bacterium identified by gut microbiota analysis of Crohn disease patients. *Proc Natl Acad Sci USA* 105: 16731–16736, 2008. doi:10.1073/pnas.0804812105.
9. **Komban RJ**, **Strömberg A**, **Biram A**, **Cervin J**, **Lebrero-Fernández C**, **Mabbott N**, **Yrlid U**, **Shulman Z**, **Bemark M**, **Lycke N.** Activated Peyer's patch B cells sample antigen directly from M cells in the subepithelial dome. *Nat Commun* 10: 2423, 2019. doi:10.1038/s41467-019-10144-w.
10. **Liu H-Y**, **Giraud A**, **Seignez C**, **Ahl D**, **Guo F**, **Sedin J**, **Walden T**, **Oh J-H**, **van Pijkeren JP**, **Holm L**, **Roos S**, **Bertilsson S**, **Phillipson M.** Distinct B cell subsets in Peyer's patches convey probiotic effects by Limosilactobacillus reuteri. *Microbiome* 9: 198, 2021. doi:10.1186/s40168-021-01128-4.

11. **Ahl D**, **Liu H**, **Schreiber O**, **Roos S**, **Phillipson M**, **Holm L.** Lactobacillus reuteri increases mucus thickness and ameliorates dextran sulphate sodium-induced colitis in mice. *Acta Physiol (Oxf)* 217: 300–310, 2016. doi:10.1111/apha.12695.
12. **Evelina V. Phillipson M**, **Roos S.** *Methods for Wound Healing*. Patent EP3237622A1. 2015 December 23.
13. **Lamb CA**, **Kennedy NA**, **Raine T**, **Hendy PA**, **Smith PJ**, **Limdi JK**, **Hayee B**, **Lomer MCE**, **Parkes GC**, **Selinger C**, **Barrett KJ**, **Davies RJ**, **Bennett C**, **Gittens S**, **Dunlop MG**, **Faiz O**, **Fraser A**, **Garrick V**, **Johnston PD**, **Parkes M**, **Sanderson J**, **Terry H**, **Gaya DR**, **Iqbal TH**, **Taylor SA**, **Smith M**, **Brookes M**, **Hansen R**, **Hawthorne AB**; **IBD guidelines eDelphi consensus group.** British Society of Gastroenterology consensus guidelines on the management of inflammatory bowel disease in adults. *Gut* 68: s1–s106, 2019. doi:10.1136/gutjnl-2019-318484.
14. **Raine T**, **Bonovas S**, **Burisch J**, **Kucharzik T**, **Adamina M**, **Annese V**, **Bachmann O**, **Bettenworth D**, **Chaparro M**, **Czuber-Dochan W**, **Eder P**, **Ellul P**, **Fidalgo C**, **Fiorino G**, **Gionchetti P**, **Gisbert JP**, **Gordon H**, **Hedin C**, **Holubar S**, **Iacucci M**, **Karmiris K**, **Katsanos K**, **Kopylov U**, **Lakatos PL**, **Lytras T**, **Lyutakov I**, **Noor N**, **Pellino G**, **Piovani D**, **Savarino E**, **Selvaggi F**, **Verstockt B**, **Spinelli A**, **Panis Y**, **Doherty G.** ECCO guidelines on therapeutics in ulcerative colitis: medical treatment. *J Crohns Colitis* 16: 2–17, 2022. doi:10.1093/ecco-jcc/jjab178.
15. **Torres J**, **Bonovas S**, **Doherty G**, **Kucharzik T**, **Gisbert JP**, **Raine T et al.** ECCO guidelines on therapeutics in Crohn's disease: medical treatment. *J Crohns Colitis* 14: 4–22, 2020. doi:10.1093/ecco-jcc/jjz180.
16. **Singh JA**, **Wells GA**, **Christensen R**, **Tanjong Ghogomu E**, **Maxwell LJ**, **MacDonald JK**, **Filippini G**, **Skoetz N**, **Francis DK**, **Lopes LC**, **Guyatt GH**, **Schmitt J**, **La Mantia L**, **Weberschock T**, **Roos JF**, **Siebert H**, **Hershan S**, **Cameron C**, **Lunn MP**, **Tugwell P**, **Buchbinder R.** Adverse effects of biologics: a network meta-analysis and Cochrane overview. *Cochrane Database Syst Rev* , 2011: CD008794, 2011. doi:10.1002/14651858.CD008794.pub2.
17. **Loftus EV**, **Feagan BG**, **Panaccione R**, **Colombel J-F**, **Sandborn WJ**, **Sands BE**, **Danese S**, **D'Haens G**, **Rubin DT**, **Shafran I**, **Parfionovas A**, **Rogers R**, **Lirio RA**, **Vermeire S.** Long-term safety of vedolizumab for inflammatory bowel disease. *Aliment Pharmacol Ther* 52: 1353–1365, 2020. doi:10.1111/apt.16060.
18. **European Medicines Agency.** *Assessment Report: Entyvio International Non-Proprietary Name: Vedolizumab*. Committee for Medicinal Products for Human Use (CHMP), 2014.
19. **Danese S**, **Furfaro F**, **Vetrano S.** Targeting S1P in inflammatory bowel disease: new avenues for modulating intestinal leukocyte migration. *J Crohns Colitis* 12: S678–S686, 2018. doi:10.1093/ecco-jcc/jjx107.
20. **Scott FL**, **Clemons B**, **Brooks J**, **Brahmachary E**, **Powell R**, **Dedman H**, **Desale HG**, **Timony GA**, **Martinborough E**, **Rosen H**, **Roberts E**, **Boehm MF**, **Peach RJ.** Ozanimod (RPC1063) is a potent sphingosine-1-phosphate receptor-1 ($S1P_1$) and receptor-5 ($S1P_5$) agonist with autoimmune disease-modifying activity: Ozanimod: a $S1P_{1,5}$ receptor agonist for autoimmune disease. *Br J Pharmacol* 173: 1778–1792, 2016. doi:10.1111/bph.13476.
21. **Squibb BL.** Zeposia (Online). FASS Vårdpersonal, 2023. https://www.fass.se/LIF/product;jsessionid=node0cwhzoixeh6kb105okk1929cv1623607.node0?npId=20190307000057&userType=0 [Accessed August 2023].
22. **Shivaji UN**, **Sharratt CL**, **Thomas T**, **Smith SCL**, **Iacucci M**, **Moran GW**, **Ghosh S**, **Bhala N.** Review article: managing the adverse events caused by anti-TNF therapy in inflammatory bowel disease. *Aliment Pharmacol Ther* 49: 664–680, 2019. doi:10.1111/apt.15097.
23. **Kaur L**, **Gordon M**, **Baines PA**, **Iheozor-Ejiofor Z**, **Sinopoulou V**, **Akobeng AK.** Probiotics for induction of remission in ulcerative colitis. *Cochrane Database Syst Rev* 3: CD005573, 2020. doi:10.1002/14651858.CD005573.pub3.
24. **Naimi A**, **Mohammed RN**, **Raji A**, **Chupradit S**, **Yumashev AV**, **Suksatan W**, **Shalaby MN**, **Thangavelu L**, **Kamrava S**, **Shomali N**, **Sohrabi AD**, **Adili A**, **Noroozi-Aghideh A**, **Razeghian E.** Tumor immunotherapies by immune checkpoint inhibitors (ICIs); the pros and cons. *Cell Commun Signal* 20: 44, 2022. doi:10.1186/s12964-022-00854-y.
25. **Portenkirchner C**, **Kienle P**, **Horisberger K.** Checkpoint inhibitor-induced colitis—a clinical overview of incidence, prognostic implications and extension of current treatment options. *Pharmaceuticals (Basel)* 14: 367, 2021. doi:10.3390/ph14040367.
26. **Hodi FS**, **Chiarion-Sileni V**, **Gonzalez R**, **Grob J-J**, **Rutkowski P**, **Cowey CL**, **Lao CD**, **Schadendorf D**, **Wagstaff J**, **Dummer R**, **Ferrucci PF**, **Smylie M**, **Hill A**, **Hogg D**, **Marquez-Rodas I**, **Jiang J**, **Rizzo J**, **Larkin J**, **Wolchok JD.** Nivolumab plus ipilimumab or nivolumab alone versus ipilimumab alone in advanced melanoma (CheckMate 067): 4-year outcomes of a multicentre, randomised, phase 3 trial. *Lancet Oncol* 19: 1480–1492, 2018. doi:10.1016/S1470-2045(18)30700-9.
27. **Nielsen DL**, **Juhl CB**, **Chen IM**, **Kellermann L**, **Nielsen OH.** Immune checkpoint Inhibitor–induced diarrhea and colitis: incidence and management. A systematic review and meta-analysis. *Cancer Treat Rev* 109: 102440, 2022. doi:10.1016/j.ctrv.2022.102440.
28. **Cooper HS**, **Murthy SN**, **Shah RS**, **Sedergran DJ.** Clinicopathologic study of dextran sulfate sodium experimental murine colitis. *Lab Invest* 69: 238–249, 1993.
29. **Vågesjö E**, **Öhnstedt E**, **Mortier A**, **Lofton H**, **Huss F**, **Proost P**, **Roos S**, **Phillipson M.** Accelerated wound healing in mice by on-site production and delivery of CXCL12 by transformed lactic acid bacteria. *Proc Natl Acad Sci USA* 115: 1895–1900, 2018. doi:10.1073/pnas.1716580115.
30. **Na YR**, **Jung D**, **Stakenborg M**, **Jang H**, **Gu GJ**, **Jeong MR**, **Suh SY**, **Kim HJ**, **Kwon YH**, **Sung TS**, **Ryoo SB**, **Park KJ**, **Im JP**, **Park JY**, **Lee YS**, **Han H**, **Park B**, **Lee S**, **Kim D**, **Lee HS**, **Cleynen I**, **Matteoli G**, **Seok SH.** Prostaglandin E_2 receptor PTGER4-expressing macrophages promote intestinal epithelial barrier regeneration upon inflammation. *Gut* 70: 2249–2260, 2021. doi:10.1136/gutjnl-2020-322146.
31. **Deguchi Y**, **Andoh A**, **Yagi Y**, **Bamba S**, **Inatomi O**, **Tsujikawa T**, **Fujiyama Y.** The S1P receptor modulator FTY720 prevents the development of experimental colitis in mice. *Oncol Rep* 16: 699–703, 2006.
32. **Karimi S**, **Ahl D**, **Vågesjö E**, **Holm L**, **Phillipson M**, **Jonsson H**, **Roos S.** In vivo and in vitro detection of luminescent and fluorescent lactobacillus reuteri and application of red fluorescent mCherry for assessing plasmid persistence. *PLoS One* 11: e0151969, 2016. doi:10.1371/journal.pone.0151969.
33. **Perez-Ruiz E**, **Minute L**, **Otano I**, **Alvarez M**, **Ochoa MC**, **Belsue V**, **De Andrea C**, **Rodriguez-Ruiz ME**, **Perez-Gracia JL**, **Marquez-Rodas I**, **Llacer C**, **Alvarez M**, **De Luque V**, **Molina C**, **Teijeira A**, **Berraondo P**, **Melero I.** Prophylactic TNF blockade uncouples efficacy and toxicity in dual CTLA-4 and PD-1 immunotherapy. *Nature* 569: 428–432, 2019. doi:10.1038/s41586-019-1162-y.
34. **Nicodeme E**, **Blandel F**, **Boullay V**, **Saintillan Y**, **Krysa G**, **Boullay A-B**, **Tousaint J-J**, **Artus R**, **Levenez L**, **Odillard J**, **Jacquet I**, **Duchamp O**, **Viviani F.** Abstract 3228: Immune checkpoint blockade and autoimmune diseases: Development of a mouse model of colitis induced by anti-CTLA-4. *Cancer Research* 79: 3228, 2019. doi:10.1158/1538-7445.AM2019-3228.
35. **Farr L**, **Ghosh S**, **Jiang N**, **Watanabe K**, **Parlak M**, **Bucala R**, **Moonah S.** CD74 signaling links inflammation to intestinal epithelial cell regeneration and promotes mucosal healing. *Cell Mol Gastroenterol Hepatol* 10: 101–112, 2020. doi:10.1016/j.jcmgh.2020.01.009.
36. **Mueller W**, **Schütz D**, **Nagel F**, **Schulz S**, **Stumm R.** Hierarchical organization of multi-site phosphorylation at the CXCR4 C terminus. *PLoS One* 8: e64975, 2013. doi:10.1371/journal.pone.0064975.
37. **Mimura-Yamamoto Y**, **Shinohara H**, **Kashiwagi T**, **Sato T**, **Shioda S**, **Seki T.** Dynamics and function of CXCR4 in formation of the granule cell layer during hippocampal development. *Sci Rep* 7: 5647, 2017. doi:10.1038/s41598-017-05738-7.
38. **Allen CDC**, **Ansel KM**, **Low C**, **Lesley R**, **Tamamura H**, **Fujii N**, **Cyster JG.** Germinal center dark and light zone organization is mediated by CXCR4 and CXCR5. *Nat Immunol* 5: 943–952, 2004. doi:10.1038/ni1100.
39. **Rodda LB**, **Bannard O**, **Ludewig B**, **Nagasawa T**, **Cyster JG.** Phenotypic and morphological properties of germinal center dark zone Cxcl12-expressing reticular cells. *J Immunol* 195: 4781–4791, 2015. doi:10.4049/jimmunol.1501191.
40. **Stebegg M**, **Kumar SD**, **Silva-Cayetano A**, **Fonseca VR**, **Linterman MA**, **Graca L.** Regulation of the germinal center response. *Front Immunol* 9: 2469, 2018. doi:10.3389/fimmu.2018.02469.
41. **Schmidt TH**, **Bannard O**, **Gray EE**, **Cyster JG.** CXCR4 promotes B cell egress from Peyer's patches. *J Exp Med* 210: 1099–1107, 2013. doi:10.1084/jem.20122574.

42. **Skribek M**, **Rounis K**, **Afshar S**, **Grundberg O**, **Friesland S**, **Tsakonas G**, **Ekman S**, **De Petris L.** Effect of corticosteroids on the outcome of patients with advanced non–small cell lung cancer treated with immune-checkpoint inhibitors. *Eur J Cancer* 145: 245–254, 2021. doi:10.1016/j.ejca.2020.12.012.
43. **Li F**, **Li X**, **Cheng CC**, **Bujdoš D**, **Tollenaar S**, **Simpson DJ**, **Tasseva G**, **Perez-Muñoz ME**, **Frese S**, **Gänzle MG**, **Walter J**, **Zheng J.** A phylogenomic analysis of *Limosilactobacillus reuteri* reveals ancient and stable evolutionary relationships with rodents and birds and zoonotic transmission to humans. *BMC Biol* 21: 53, 2023. doi:10.1186/s12915-023-01541-1.
44. **Mu Q**, **Tavella VJ**, **Luo XM.** Role of *Lactobacillus reuteri* in human health and diseases. *Front Microbiol* 9: 757, 2018. doi:10.3389/fmicb.2018.00757.
45. **Ihara S**, **Hirata Y**, **Koike K.** TGF-β in inflammatory bowel disease: a key regulator of immune cells, epithelium, and the intestinal microbiota. *J Gastroenterol* 52: 777–787, 2017. doi:10.1007/s00535-017-1350-1.
46. **Quiros M**, **Nishio H**, **Neumann PA**, **Siuda D**, **Brazil JC**, **Azcutia V**, **Hilgarth R**, **O'Leary MN**, **Garcia-Hernandez V**, **Leoni G**, **Feng M**, **Bernal G**, **Williams H**, **Dedhia PH**, **Gerner-Smidt C**, **Spence J**, **Parkos CA**, **Denning TL**, **Nusrat A.** Macrophage-derived IL-10 mediates mucosal repair by epithelial WISP-1 signaling. *J Clin Invest* 127: 3510–3520, 2017. doi:10.1172/JCI90229.
47. **Xue X**, **Falcon DM.** The role of immune cells and cytokines in intestinal wound healing. *Int J Mol Sci* 20: 6097, 2019. doi:10.3390/ijms20236097.
48. **Dodd JH**, **Jordan R**, **Koplpwitz B**, **Koplowitz LP**, **Spana C.** Efficacy of the Melanocortin Receptor Agonist PL8177 as a Potential Therapy for Gastrointestinal Inflammatory Diseases (Online). Chicago: Digestive Disease Week, 2023.
49. **Sandborn WJ**, **Peyrin-Biroulet L**, **Zhang J**, **Chiorean M**, **Vermeire S**, **Lee SD**, **Kühbacher T**, **Yacyshyn B**, **Cabell CH**, **Naik SU**, **Klassen P**, **Panés J.** Efficacy and safety of etrasimod in a phase 2 randomized trial of patients with ulcerative colitis. *Gastroenterology* 158: 550–561, 2020. doi:10.1053/j.gastro.2019.10.035.
50. **Rutter JW**, **Dekker L**, **Owen KA**, **Barnes CP.** Microbiome engineering: engineered live biotherapeutic products for treating human disease. *Front Bioeng Biotechnol* 10: 1000873, 2022. doi:10.3389/fbioe.2022.1000873.
51. **Charbonneau MR**, **Isabella VM**, **Li N**, **Kurtz CB.** Developing a new class of engineered live bacterial therapeutics to treat human diseases. *Nat Commun* 11: 1738, 2020. doi:10.1038/s41467-020-15508-1.
52. **Öhnstedt E**, **Lofton Tomenius H**, **Frank P**, **Roos S**, **Vågesjö E**, **Phillipson M.** Accelerated wound healing in minipigs by on-site production and delivery of CXCL12 by transformed lactic acid bacteria. *Pharmaceutics* 14: 229, 2022. doi:10.3390/pharmaceutics14020229.
53. **Öhnstedt E**, **Vågesjö E**, **Fasth A**, **Lofton Tomenius H**, **Dahg P**, **Jönsson S**, **Tyagi N**, **Åström M**, **Myktybekova Z**, **Ringstad L**, **Jorvid M**, **Frank P**, **Hedén P**, **Roos S**, **Phillipson M.** Engineered bacteria to accelerate wound healing: an adaptive, randomised, double-blind, placebo-controlled, first-in-human phase 1 trial. *eClinicalMedicine* 60: 102014, 2023. doi:10.1016/j.eclinm.2023.102014.
54. **Dougan M**, **Wang Y**, **Rubio-Tapia A**, **Lim JK.** AGA clinical practice update on diagnosis and management of immune checkpoint inhibitor colitis and hepatitis: expert review. *Gastroenterology* 160: 1384–1393, 2021. doi:10.1053/j.gastro.2020.08.063.
55. **Siakavellas SI**, **Bamias G.** Checkpoint inhibitor colitis: a new model of inflammatory bowel disease? *Curr Opin Gastroenterol* 34: 377–383, 2018. doi:10.1097/MOG.0000000000000482.
56. **Bertrand F**, **Montfort A**, **Marcheteau E**, **Imbert C**, **Gilhodes J**, **Filleron T**, **Rochaix P**, **Andrieu-Abadie N**, **Levade T**, **Meyer N**, **Colacios C**, **Ségui B.** TNFα blockade overcomes resistance to anti-PD-1 in experimental melanoma. *Nat Commun* 8: 2256, 2017. doi:10.1038/s41467-017-02358-7.